International Journal of Fluid Machinery and Systems
Vol. 3, No. 2, April-June 2010

Original Paper

Cavitation in Pump Inducer with Axi-asymmetrical Inlet Plate Observed by Multi-cameras

Jun-Ho Kim[1], Takashi Atono[2], Koichi Ishizaka[3], Satoshi Watanabe[3] and Akinori Furukawa[3]

[1] Hydro Research Part / R&D Center, Hyosung EBARA Co., Ltd. Changwon Plant, 43-1 Ungnam-dong, Changwon-si, Gyeongsangnam-do 641-290, Korea, hec-kjh@hyosung.com
[2] Department of Processing Information Engineering, Kyushu Polytechnic College, 1665-1 Shii, Kokurakita-ku, Kitakyushu 802-0985, Japan, atono@kyushu-pc.ac.jp
[3] Department of Mechanical Engineering Science, Kyushu University, 744 Motooka, Nishi-ku, Fukuoka 819-0395, Japan, ishizk@mech.kyushu-u.ac.jp, fmnabe@mech.kyushu-u.ac.jp, fmfuru@mech.kyushu-u.ac.jp

Abstract

The attachment of inducer in front of main impeller is a powerful method to improve cavitation performance; however, cavitation surge oscillation with low frequency occurs with blade cavity growing to each throat section of blade passage simultaneously. Then, one conceptual method of installing suction axi-asymmetrical plate has been proposed so as to keep every throat passage away from being unstable at once, and the effect on suppression of the oscillation were investigated. In the present study, cavitation behaviors in the inducer is observed with distributing multi-cameras circumferentially, recording simultaneously and reconstructing multi-photos on one plane field as moving a linear cascade. Observed results are utilized for discussion with other measuring results as casing wall pressure distribution. Then the suppression mechanism of oscillation by installing axi-asymmetrical inlet plate will be clarified in more details.

Keywords: Pump inducer, Cavitation surge suppression, Axi-asymmetrical inlet plate, Multi-cameras observation system

1. Introduction

Recently, the miniaturization of turbopumps has been expected to reduce the pump space for various industrial fields, therefore that results in the pump high-speed operation. The installation of inducer just upstream of main impeller is known to be an efficient way to achieve the high cavitation performance for turbopumps, since an inducer is able to keep the high headrise performance even in severe cavitating conditions due to high-speed pump operation [1][2][3].

However, the serious cavitation instability, called as cavitation surge oscillation [4], has been known to occur in a certain pump operation with partial flow rate and low suction condition, and has happened to lead the pump system in harmful operation resonated with the frequency of surge fluctuation. It was shown in our former work [5] that cavitation surge with low frequency appears when all cavities on suction blade surface of the inducer expand and reach synchronously to throat section of blade passages along with decreasing suction pressure, and fluctuating tails of cavity excite every blade passage to be unstable.

Then we have made a conceptual attempt to force distorted inlet flow and avoid every blade cavity developing simultaneously into throat section of blade passage by installing an axi-asymmerical obstacle upstream to inducers, that was effective to reduce the cavitation surge region of widely used inducers [6]. In the present study, the observation by the aid of 5 CCD image cameras positioned peripherally on a constant half circle around inducer casing was focussed on to reveal cavitation behaviors on every blade of inducer passing by the obstacle plate, then discussed how the cavitation surge was suppressed by the axi-asymmetric obstacle plate to refer the pressure distributions on casing wall measured by widely arrayed high response sensors.

2. Effect on the suppression of cavitation surge by installing the axi-asymmetrical inlet plate

Figures 1 and 2 show a closed water flow loop used and a cross-sectional view of test apparatus from the part of inlet contraction upstream to inducer section (with the mounted inlet obstacle plate) to the part of guide vanes downstream, respectively. The suction pipe has the inner diameter of 125mm and the length of 9.5m from the tank to the upstream straight vanes and the

Received April 16 2009; accepted for publication May 10 2010: Review conducted by Dr. Tadashi Tanuma. (Paper number O09010)
Corresponding author: Akinori Furukawa, Professor, fmfuru@mech.kyushu-u.ac.jp

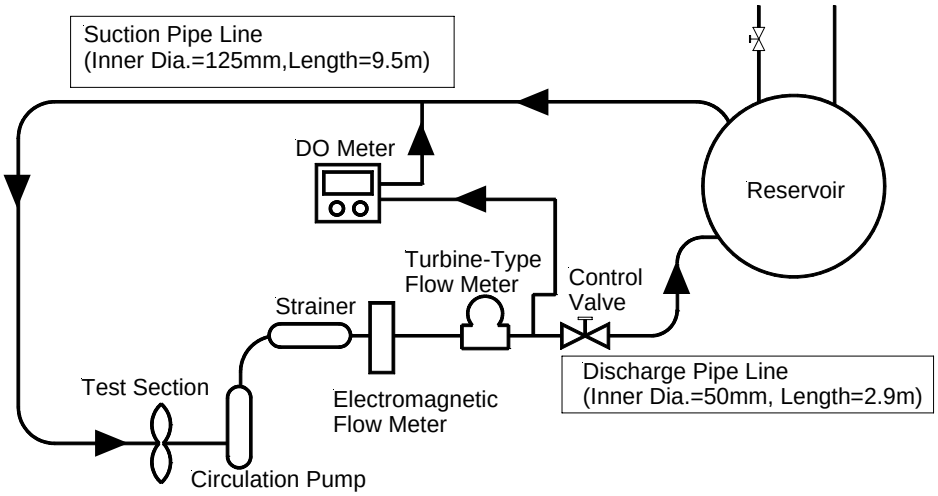

Fig. 1 Test loop of water flow

discharge pipe has 50mm diameter and 2.9m length from the water circulation (booster) pump outlet to the tank. On the discharge piping line, a strainer, an electromagnetic flow meter, a turbine-type one and a control valve are installed. The booster pump was operated when the inducer head is not high enough to circulate water in the loop. It is verified experimentally that the booster pump operation has no influence on the cavitation surge phenomena of inducers.

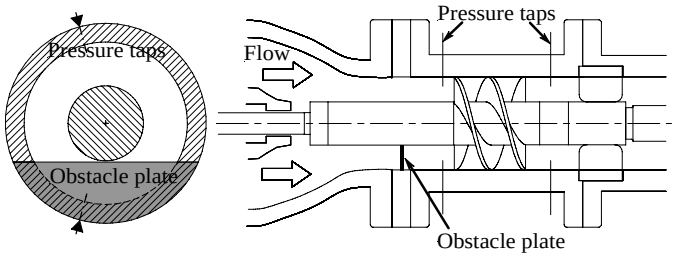

Obstacle plate (BP027)

Fig. 2 Schematic view of test section and obstacle plate [6]

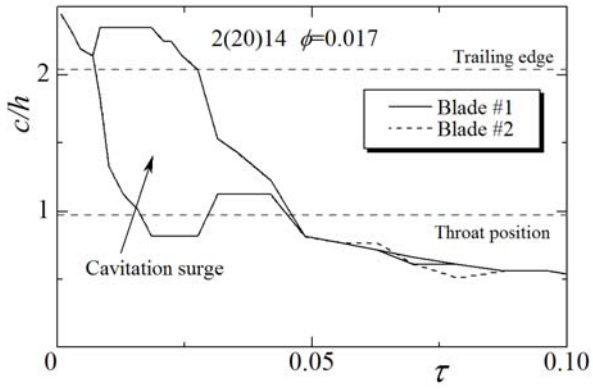

Fig. 3 Change of blade cavity length in inducer without BP027 at ϕ = 0.017 [6]

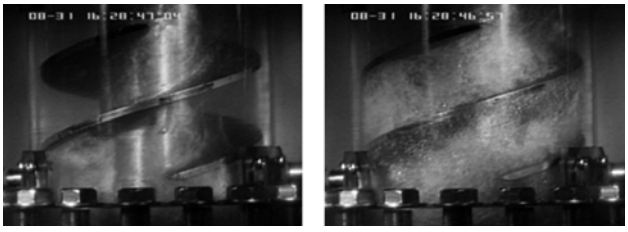

(a) Shrunk blade cavity (b) Spread blade cavity

Fig. 4 Cavity behavior in cavitation surge oscillation at τ = 0.02 and ϕ = 0.017

The test inducer is a flat plate helical type with blade number of 2, tip solidity of 2.0, blade tip angle of β_t =14 deg, blade tip diameter of D = 64 mm and hub-tip ratio of 0.47. The tip clearance between blade tip and suction casing surface is 0.5 mm [5]. Cavitation tests were performed as decreasing the suction pressure of NPSH under the constant rotational speed of N = 5000 min^{-1} (or 3000min^{-1} under the similitude for operation during observing cavitation behaviors by multi-cameras system as depicted at the following section) and the constant mean flow rate. During the tests, the casing wall pressures were measured at the inlet and the outlet of inducer (as pressure taps indicated in Fig.2) to sense unstable pressure fluctuations approaching, and also the changing blade cavities on each suction blade surface of inducer were recorded by video equipment. As the example [6], the observed cavity lengths on inducer blades are shown in Fig.3 as decreasing NPSH under flow coefficient of ϕ = 0.017. Under unstable cavitation conditions, each blade cavity lengths were observed in resulted oscillatory manner, then each peak values between the most spreading and the most shrinking phases were representatively indicated as every split branch of line in the figure. Each parameter was defined as follows, flow coefficient of $\phi = Q/AU_t$ (Q: flow rate, A: cross-sectional area of flow passage, U_t: blade tip peripheral speed), dimensionless NPSH of τ (= gH_{sv}/U_t^2 , g: gravity, H_{sv}: = NPSH), and c/h denotes the ratio of c (length of blade cavity along the blade surface) to h (blade spacing).

It is shown in Fig.3 that the operation of inducer fails into cavitation surge condition, when each tail of blade cavity reaches to

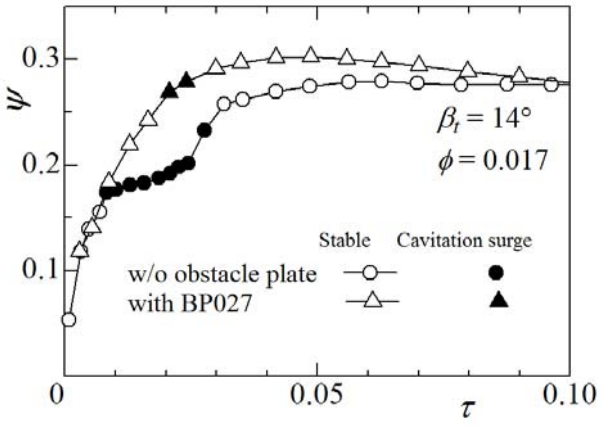

Fig. 5 Change of cavitation performance with BP027 setting [6]

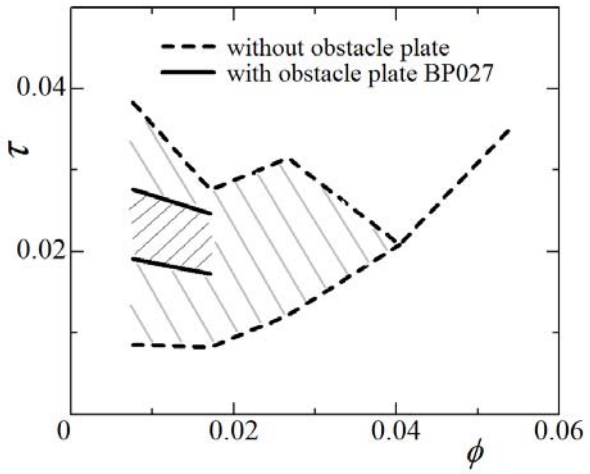

Fig. 6 Onset region of cavitation surge oscillation [6]

the throat section of blade passage. Figure 4 represents both typical views in the phase of surge condition, as (a) the state of shrunk blade cavity accompanied with strong back-flow and (b) the state of spread cavity almost to the blade trailing edge. In this case, the behavior of blade cavities was oscillated among two phases of view, and the frequency of oscillatory manner was kept statistically stable in 2 Hz. Then the axi-asymmetrical obstacle plate was installed upstream of 0.555*D* (*D*: inner diameter of inducer casing) to inducer inlet, and examined to affect on the deduction of cavitation surge as shown in Fig.6. The obstacle plate narrows the cross-sectional passage of inducer inlet by the ratio of 26.5% (then the plate denoted as BP027 hereafter). Figure 5 indicates the difference between each cavitation characteristics at flow rate of ϕ=0.017 without or with the installation of obstacle plate. The onset region of cavitation surge, resulted from cavitation tests with the obstacle plate, is compared with that of tests not installed in Fig.6. The onset of cavitation surge was defined by observing the wall pressure at inducer outlet, whenever the apparently stable peak of low frequency on analyzed spectrum appears and exceeds that of blade passing frequency (BPF) without cavitation at the same flow rate. The periodic behaviors of blade cavities were observed by the aid of hi-speed video camera, and confirmed to coincide with the wall pressure measurement. As shown in Fig.5, the operation points (symbol ▲: τ = 0.02~0.025) of cavitation surge occurring in the setup installed the obstacle plate were apparently narrower than those (symbol ●: τ = 0.01~0.03) of bare setup without plate at flow rate of ϕ=0.017. Also as found in Fig.6, the onset region of cavitation surge over entire flow range as indicated by the split branches of line was fairly reduced in the case of setup with the plate both range for suction condition τ and flow rate ϕ.

3. Observation of cavitation behavior by simultaneous multi-cameras system

In this section, the dynamic behavior of cavitation observed by multi-cameras system will be expressed as a sequence of pictures during one periodic rotation, and also referred to the pressure measurement on the casing wall by high response pressure sensors when the axi-asymmetric obstacle plate installed upstream to an inducer.

First of all, we have to explain a schematic outline of multi-cameras system. As essentially, the setup of the obstacle plate is intended to distort the incoming flow to an inducer, which makes the state of cavity different on each blade passage, then enables to prevent the whole inlet throat sections of blade passages from being choked simultaneously. In order to discuss the suppression effect of installing the axi-asymmetrical obstacle plate, the relation between the flow distortion and the difference of cavitation behaviors in peripherally different sides with/without obstacle plate would be required. So a certain device to obtain peripherally instantaneous and entire view of cavitation behavior over 360 deg range around the inducer is necessary to depict the suppression effect of the obstacle plate. But at the present stage of the test apparatus for this examination, it is too small to distribute sufficient optical devices such as cameras and lighting equipments over 360 deg range. The following idea was applied. After several tests, being confirmed that observed blade cavities were quite similar in every corresponding suction condition, the next substitutive scheme with the multi-cameras observation system as shown in Fig.7 was attempted to assemble two halves of peripheral view over 180 deg into a panoramically entire view around the inducer. For a half of view, 5 CCD-cameras were distributed

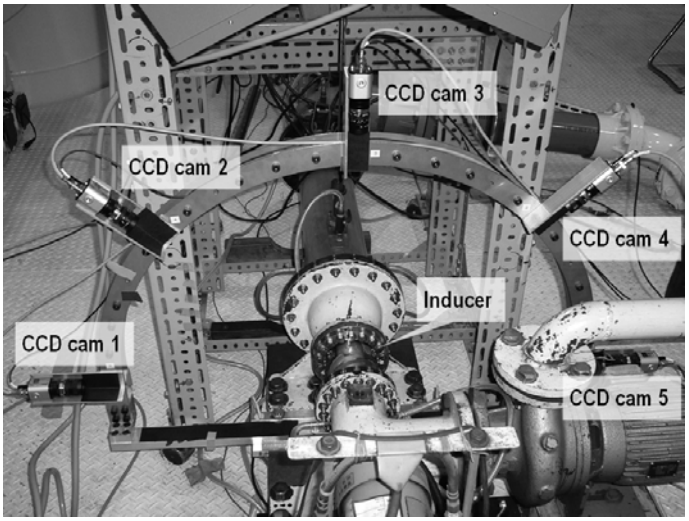

Fig. 7 Multi-cameras observation system

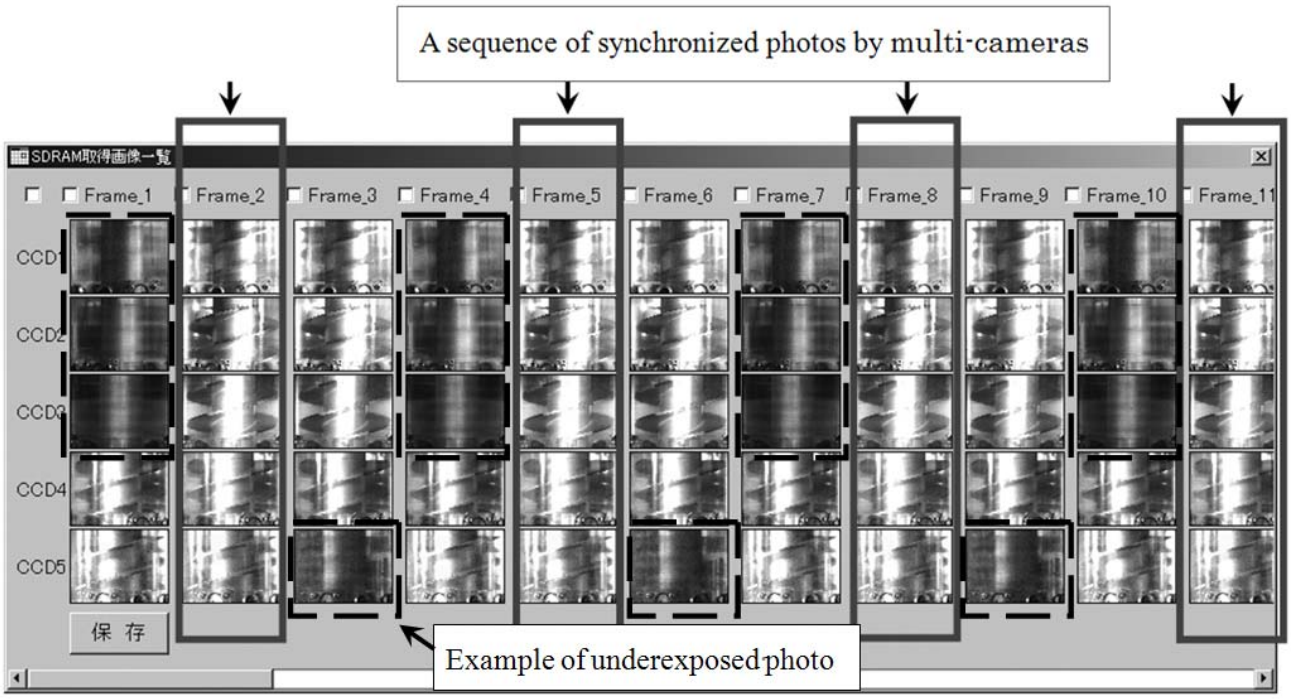

Fig. 8 Instantaneously recorded photos with multi-cameras

peripherally in every 45 deg around the inducer. Once the half view was observed and simultaneously recorded, another half was subsequently obtained after assembling the obstacle plate to the opposite side instead of shifting the cameras to the mirror image position. In the present observation, every video camera with recording rate of 30 fps (normal) was used as a synchronous still camera with help of stroboscopic-lights. The stroboscopic-lights were driven to flash at the fixed relative positions of obstacle to inducer blades per one shaft rotation. Need to say as an artificial problem, the trigger signal to drive stroboscopic-lights at one period of shaft rotation (signal rate 83.3 Hz at N = 5000 min^{-1} of shaft rotation) is too fast for normal frame rate of recording to eliminate some happened duplication of different two frames, therefore one half divisor output signal to the original signal of rotation was adapted to record only single frame at every circumferential pose of 10 deg relatively to the obstacle plate. For example, Figure 8 shows several pictures simultaneously recorded by 5 CCD-cameras in a certain pose of the inducer. In this figure, five pictures arrayed in each column were recorded in a same instant, and those in each line were obtained in another time histories. The shaded pictures in Fig.8 (as indicated in broken lined frames) come from underexposure in the interlace time because of the reduced trigger signal. By every relative pose to the obstacle, ten sets which consist of valid five pictures in the same instant as shown Fig.8 were picked up. To reduce unsteady behavior in recorded pictures, a time-averaged picture was processed in the procedure of graphical accumulation by every pixel of each picture (as shown in Fig.9(a)). But the averaged pictures tend to show dull contours of blade cavities, so one picture of each set of ten, that resembled the averaged picture, was accepted as a real best sample (an example is shown in Fig.9(b)). As seen in Fig.9, a part of picture surrounded with dotted line in a frame was selected as a valid and flat view for each CCD-camera. Five selected pictures, which were taken simultaneously, were connected each other to obtain the peripheral view of instantaneous cavitation behavior over 180 deg. After the other peripheral view over 180 deg. in opposite side under the same condition was obtained, a panoramic still picture over 360 deg is completed by putting them together.

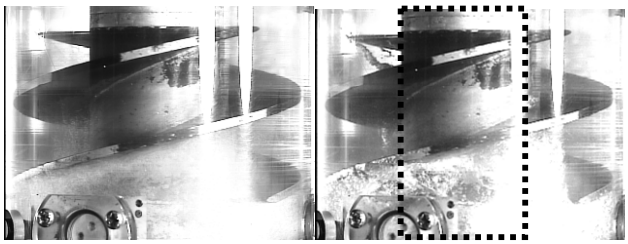

(a) Averaged photo by graphical process (b) Selected instant photo close to the averaged

Fig. 9 Selection of referred photo

Finally, in a target suction condition, we obtained thirty-six panoramic still pictures at the corresponding poses of the inducer to the obstacle plate in one revolution. Those pictures were utilized to make a movie that expresses the dynamic behavior of blade cavities on the relatively moving linear cascades around the obstacle plate.

As a typical result before cavitation surge condition at ϕ = 0.017, and τ = 0.045, several panoramic still pictures taken at different poses of two-bladed inducer to the axi-asymmetrical obstacle are shown in Fig.10. Each denoted angle of blade position in Fig.10(a)~(d) was based on the position 0 deg that the referred blade leading (blade #2) of cascades was passing just by the center of the obstacle's arc. The flow direction through cascades is right upward from the left bottom-side in those pictures and the the blade leading and trailing edges were indicated with tiny arrows in pictures. Blade cavity, the end of which is emphasized with dotted line in the picture, is elongated from the blade leading edges along with the suction surface. The change of blade cavities length in concern was supposed to depend on the relative position of blade leading edge to the axi-asymmetrical obstacle plate and

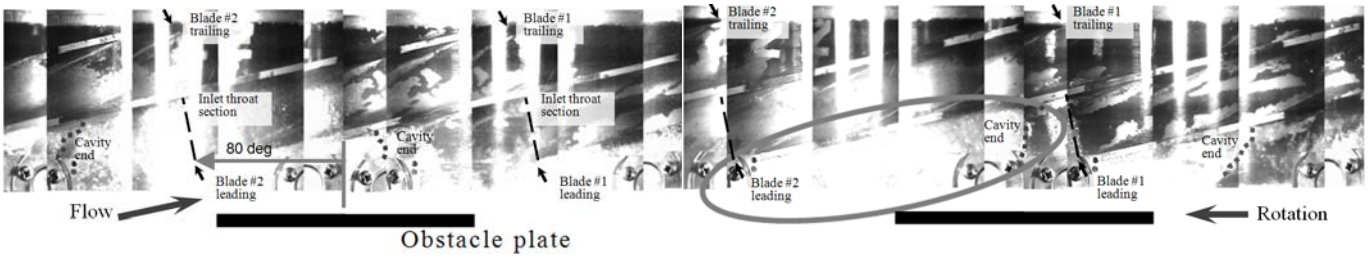

(a) Blade position 80 deg

(b) Blade position 150 deg (longest cavity in circle)

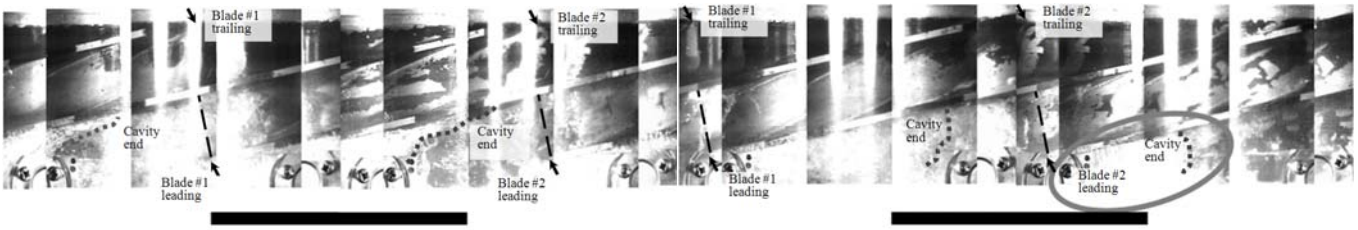

(c) Blade position 250 deg

(d) Blade position 350 deg (shortest cavity in circle)

Fig. 10 360 deg panorama photos in case with BP027 at τ = 0.045 and ϕ = 0.017

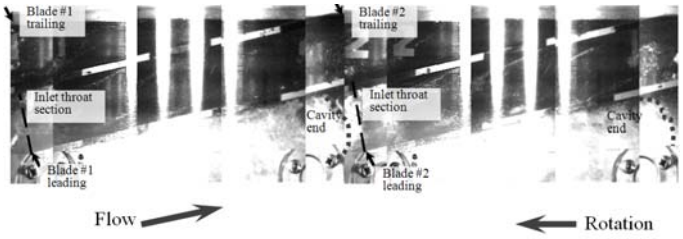

Fig. 11 360 deg panorama photos in case without BP027 at τ = 0.045 and ϕ = 0.017

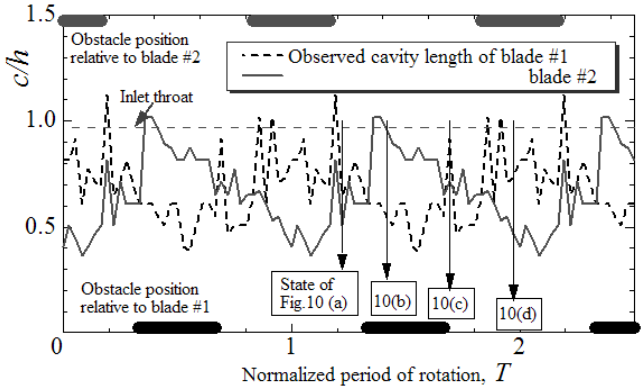

Fig. 12 Time variation of cavity length in each revolution of inducer

to be oscillatory in a period of rotation. In this case, the cavity length of blade #2 in attention was observed in the longest state as shown in the circle of Fig.10(b), and on the contrary in the shortest state of Fig.10(d). From these panoramic still pictures, changes of cavity length on both blades, blade #1 and blade #2 in one revolution were obtained as shown in Fig.12. Then meaningful results might be shown to consider the effect of the axi-aymmetrical obstacle plate on cavitation surge oscillation.

In the case without obstacle plate a panoramic still picture was recorded by the same procedure. In order to compare the cavity behavior in Fig.10, the panoramic still picture in the same suction condition at ϕ = 0.017 and τ =0.045 as Fig.10 is illustrated in Fig.11. This picture reveals that both tails of cavities on the suction surface of two blades were located at the almost same positions. It is known that the tail is approaching to reach to the throat section of blade passages at the state just before oscillation.

Figure 12 shows the change in observed cavity length of each blade derived from the former results (Fig.10). T on the horizontal axis is the dimensionless time normalized by the period of rotation. The fat-dashed lines on the both horizontal axes point out the corresponding terms in when the blade leadings were behind the obstacle plate. Referring to the pictures in Fig.10, it is clarified that the cavity length of blade #2 in concern was in a shortest state (a corresponding scene shown in

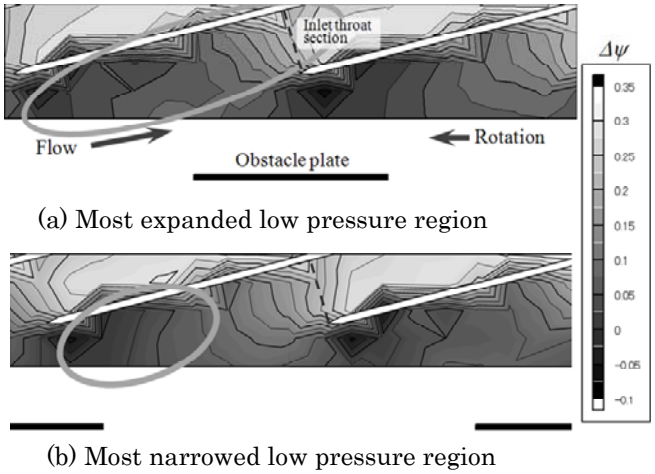

(a) Most expanded low pressure region

(b) Most narrowed low pressure region

Fig. 13 Contour map of static headrise distribution on casing wall

the circle of Fig.10(d)) whenever it's blade leading edge was passing by the center of the obstacle's arc (it's throat portion configured with the behind neighbor blade was in the open side of the obstacle), on the contrary the cavity length of blade #2 was in a longest state (a corresponding scene shown in the circle of Fig.10(b)) whenever it's blade leading edge was away from the obstacle. Although every indicated change of cavity length was so scattered and complicated in detail, each blade cavity of tested two-bladed inducer was alternatively changing its length around the obstacle plate. Through the observations by multi-cameras in this paper, the reason that the axi-asymmetrical obstacle made an effective role to reduce the cavitation surge oscillation mainly depends on the fact that when the one throat portion of blade passages was choked with own blade cavity, the another throat was forced to be out of phase with the choked passage by the obstacle plate.

Next, the pressure measurements on casing wall were carried out to understand the relationship between the cavity behavior and the circumferential position to the obstacle plate. The measurements were carried out in the procedure of moving pressure transducers arrayed in line on casing wall relatively around the obstacle plate by 20 deg and assembling each pressure distribution indexed positions to the obstacle from 18 sets of time-averaged data by phase-locked sampling. In Fig.13, the reference results (at ϕ =0.017, τ =0.30 in high NPSH condition without cavitation) are shown as an example. When one throat portion of blade passages (shown in the circle of Fig.13(a)) was behind the obstacle plate (correspond to same relative position in Fig.10(b)), the tendency that the low pressure zone behind the obstacle expanded into the throat portion of blade passage led to mostly spread the blade cavity as observed above. On the other hand, when the throat (shown in the circle of Fig.13(b)) was in open side of the obstacle (correspond to same relative position in Fig.10(d)), the low pressure zone upstream to the uncovered throat was narrow, so the blade cavity was shrunk. The foregoing is illustrated simply as a cross-sectional inlet view of inducer in Fig.14.

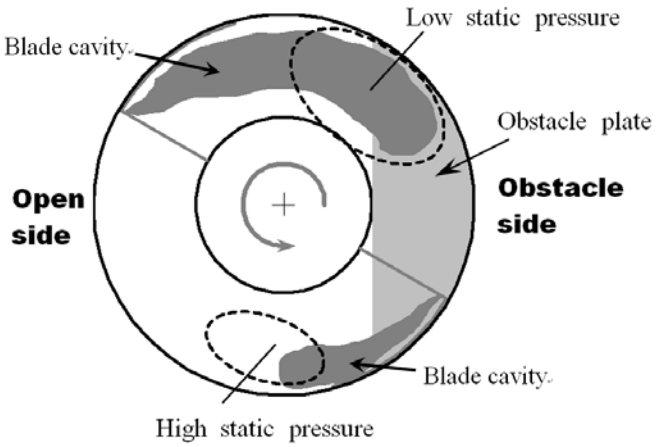

Fig. 14 Change of blade cavity length with inducer position relative to obstacle plate

4. Conclusion

Effect of installing an axi-asymmetric obstacle plate upstream of inducer on the reduction of cavitation surge phenomenon was experimentally investigated with the help of panoramic observation by multi-cameras system.

The major effect of the axi-asymmetrical obstacle plate on reducing the cavitation surge was confirmed in the fact that each blade cavity was forced to be alternatively oscillated by the obstacle, and then the choking with blade cavities in whole throat portions of blade passages was found hard to coincide.

Acknowledgments

Finally, authors should mention with their thanks that a part of this research was financially supported by the Grant-in-Aid from of Education, Sports, Culture, Science and Technology (No. 17360081) and the Scholarship of Harada Memorial Foundation.

Nomenclature

A	Cross-section area of inducer inlet [m^2]	NPSH	Net positive suction head [m]
c	Length of blade cavity [m]	Q	Flow rate [m^3/s]
D	Inner diameter of inducer casing [m]	T	Dimensionless time normalized by inducer's period of rotation
D_t	Tip blade diameter of inducer [m]	U_t	Tip peripheral speed [m/s]
g	Gravity [m^2/s]	β_t	Tip blade angle [deg]
h	Blade spacing [m]	τ	Dimensionless NPSH (= gH_{sv}/U_t^2)
Δh	Increment of static headrise on casing wall [m]	ϕ	Flow coefficient (= Q/AU_t)
H	Inducer headrise [m]	ψ	Headrise coefficient (= gH/U_t^2)
H_{sv}	(= NPSH) [m]	$\Delta\psi$	Increment of static headrise coefficient in casing wall (= $g\Delta h/U_t^2$)
L	Distance between the obstacle plate and the blade leading edge [m]		
N	Rotational speed of inducer [min^{-1}]		

References

[1] Acosta, A. J., 1958, “An Experimental Study of Cavitating Inducers, Proc. 2nd Symp. Naval Hydrodynamics,” ONR/ACR-38, (1958), pp. 537-557.
[2] Jacobsen, J. K., 1971, “Liquid Rocket Engine Turbo-pump Inducers,” NASA SP-8052.
[3] Takamatsu, Y., Furukawa, A. and Ishizaka, K., 1984, “Method of Estimation of Required NPSH of Centrifugal Pump with Inducer,” Proc. 1st China-Japan Joint Conference on Hydraulic Machinery and Equipment, pp. 253-261.
[4] Kamijo, K., Yoshida, M. and Tsujimoto, Y., 1993, “Hydraulic and Mechanical Performance of LE-7 LOX Pump Inducer,” AIAA Journal of Propulsion and Power, Vol.9, pp. 819-827.
[5] Furukawa, A., Atono, T., Ishizaka, K., Watanabe, S., 2004, “Experimental Study of Cavitation Induced Oscillation in Flat Plate Helical Inducer with Various Blade Angles,” Trans.JSME, 70-697, pp. 2325-2331 (in Japanese).
[6] Watanabe, S., Enomoto, N., Ishizaka, K., Furukawa, A., Kim, J.-H., 2004, “Suppression of Cavitation Surge of a Helical Inducer Occurring in Partial Flow Conditions,” Turbomachinery, 32-2, pp. 94-100 (in Japanese).